

Characterizing Antibody-Drug Conjugates and Assigning Drug Conjugation Sites

Using the Agilent 1290 Infinity II 2D-LC Solution Combined with the Agilent 6530 Quadrupole Time-of-Flight LC/MS System

Application Note

Biopharmaceuticals

Authors

Koen Sandra, Gerd Vanhoenacker,
Mieke Steenbeke, Isabel Vandenheede,
and Pat Sandra

Research Institute for Chromatography
(RIC)

President Kennedypark 26
B-8500 Kortrijk
Belgium

Sonja Schneider and Udo Huber
Agilent Technologies, Inc.
Waldbronn, Germany

Abstract

Antibody-drug conjugates (ADCs) are a promising new class of biopharmaceuticals. However, ADCs have a structural complexity that drives state-of-the-art chromatography and mass spectrometry to its limits. This Application Note describes how drug conjugation sites can be assessed in a highly elegant manner using comprehensive 2D-LC (RPLC×RPLC) and high-resolution mass spectrometry. An Agilent 1290 Infinity II 2D-LC Solution was combined with an Agilent 6530 Quadrupole Time-of-Flight LC/MS System.



Agilent Technologies

Introduction

Monoclonal antibodies (mAbs) have emerged as important biopharmaceuticals^{1,2}. The successes of mAbs have triggered the development of various next-generation formats. In oncology, antibody-drug conjugates (ADCs) are particularly promising because they synergistically combine a specific mAb linked to a biologically active cytotoxic drug through a stable linker³⁻⁵. Currently, two ADCs are marketed, brentuximab vedotin (Adcetris) and ado-trastuzumab emtansine (Kadcyla), and over 30 are in clinical trials³⁻⁵. From a structural point of view, ADCs possess an unsurpassed complexity because the heterogeneity of the initial antibody is superimposed with the variability of the conjugation strategy. Conjugation typically takes place on the amino groups of lysine residues or on the sulfhydryl groups of interchain cysteine residues as is the case with ado-trastuzumab emtansine and brentuximab vedotin, respectively (Figure 1). With 80–100 lysine and only eight interchain cysteine residues available, lysine conjugation yields a more heterogeneous mixture of species compared to cysteine conjugation despite the similar overall level of drugs incorporated per antibody (between zero and eight with an average of three to four)³⁻⁵.

In analyzing these molecules, all typical mAb structural characteristics need to be determined, for example, amino acid sequence and composition, molecular weight, N-glycosylation, N- and C-terminal processing, S–S bridges, free cysteine residues, deamidation, aspartate isomerization, oxidation or clipping, and sequence variants. In addition, critical quality attributes also need to be revealed such as drug-to-antibody ratio (DAR), drug distribution, and conjugation sites. This Application Note demonstrates how the Agilent 1290 Infinity II 2D-LC Solution, operated in LC×LC mode, combined with an Agilent 6530 Quadrupole Time-of-Flight (Q-TOF) LC/MS system is a powerful tool to assess drug conjugation sites.

Online two-dimensional liquid chromatography (2D-LC) is an emerging analytical tool in biopharmaceutical analysis⁶. In contrast to one-dimensional LC, 2D-LC and especially comprehensive 2D-LC (LC×LC) can substantially increase the chromatographic peak capacity if the two dimensions are orthogonal and the separation obtained in the first dimension is maintained upon transfer to the second dimension. In recent years, LC×LC has been used successfully in peptide mapping⁷⁻¹¹.

Experimental

Materials

Acetonitrile, methanol, formic acid, and water were acquired from Biosolve (Valkenswaard, The Netherlands). Trifluoroacetic acid, dithiothreitol (DTT), iodoacetamide (IAM), ammonium bicarbonate, and phosphoric acid were purchased from Sigma-Aldrich (St. Louis, MO, USA), and porcine sequencing grade modified trypsin from Promega (Madison, MA, USA). Tris-HCl was from Thermo Fisher Scientific (Waltham, MA, USA), and Rapigest from Waters (Milford, MA, USA). Herceptin and Kadcyla were from Roche (Basel, Switzerland), and Adcetris from Seattle Genetics (Seattle, WA, USA).

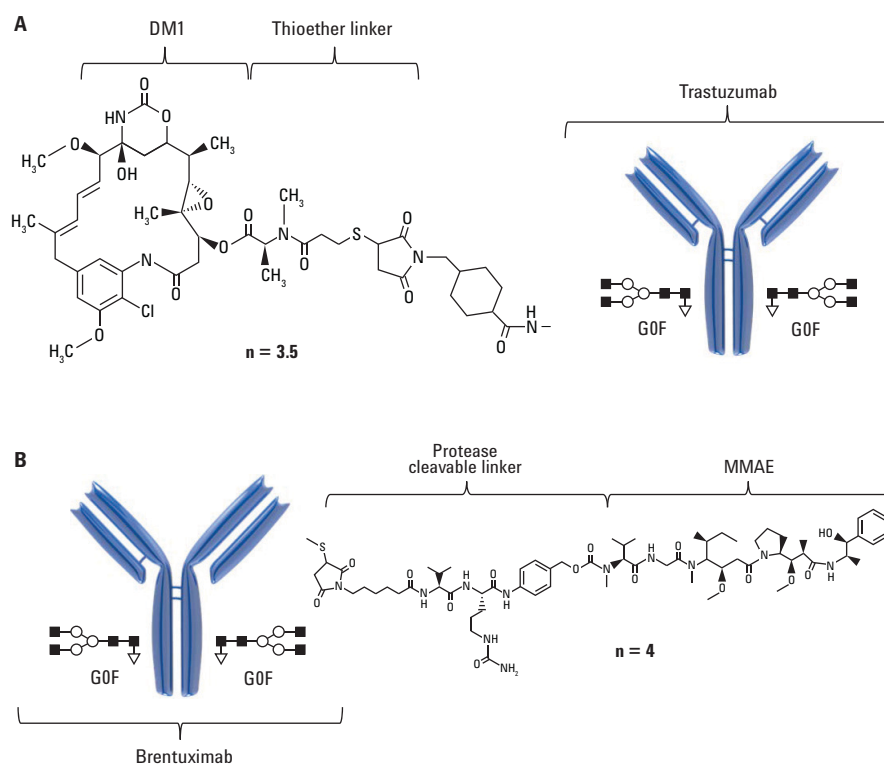


Figure 1. A) Anatomy of ado-trastuzumab emtansine (Kadcyla), which combines the anti-HER2 antibody trastuzumab (Herceptin) with the cytotoxic microtubule-inhibiting maytansine derivative DM1 conjugated to lysine residues through a nonreducible thioether linker. DM1 is conjugated with an average of 3.5 drugs per antibody. B) Anatomy of brentuximab vedotin (Adcetris) which combines the anti-CD30 antibody brentuximab with the antimetabolic drug monomethylauristatin E (MMAE) conjugated to interchain cysteine residues through a cathepsin-cleavable valine-citrulline linker. MMAE is conjugated with an average of 4.0 drugs per antibody.

Sample preparation

To a volume corresponding to 100 µg of protein, 105 µL of 0.1 % Rapigest in 100 mM Tris-HCl pH 8 was added, followed by the addition of 100 mM Tris-HCl pH 8 to a final volume of 192.5 µL. The sample was then reduced at 60 °C for 30 minutes by the addition of 5 mM DTT (2.5 µL of 400 mM DTT in 100 mM Tris-HCl), and alkylated at 37 °C for 1 hour by adding 10 mM IAA (5 µL of 400 mM IAA in 100 mM Tris-HCl). Digestion proceeded for 16 hours at 37 °C using trypsin as protease added at an enzyme-to-substrate ratio of 1:25 (w:w). Lyophilized trypsin (20 µg) dissolved in 100 mM Tris-HCl (50 µL) was added in a volume of 10 µL, giving rise to a final sample volume of 210 µL.

2D-LC instrumentation

An Agilent 1290 Infinity II 2D-LC Solution with the following configuration was used:

- Agilent 1290 Infinity II High Speed Pump with seal wash option (first dimension) (G7120A)
- Agilent 1290 Infinity II High Speed Pump (second dimension) (G7120A)
- Agilent 1290 Infinity II Multisampler (G7167B)
- Agilent 1290 Infinity II Multicolumn Thermostat (G7116B)
- Agilent 1290 Infinity Valve Drive (G1170A)
- Agilent 2-position/4-port duo-valve for 2D-LC equipped with two 40-µL loops (G4236A)
- Agilent 6530 Accurate-Mass Quadrupole Time-of-Flight LC/MS system (G6530A)

LC×LC method parameters

RPLC×RPLC	
First dimension	
Column	Agilent ZORBAX Bonus-RP, 2.1 × 150, 3.5 µm
Solvent A	10 mM NH ₄ HCO ₃ , pH 8.2
Solvent B	MeOH:ACN 50:50
Flow rate	80 µL/min
Gradient	0 to 45 minutes – 2 to 92 %B 45 to 46 minutes – 92 to 100 %B 46 to 55 minutes – 100 %B Post time – 9 minutes at 2 %B
Temperature	23 °C
Second dimension	
Column	Agilent ZORBAX Eclipse Plus C18, 4.6 × 50 mm, 3.5 µm
Solvent A	0.1 % H ₃ PO ₄ in water (UV) or 0.1 % HCOOH in water (MS)
Solvent B	ACN
Flow rate	3.5 mL/min
Idle flow rate	0.5 mL/min
Initial gradient	0 to 0.35 minutes – 2 to 10 %B 0.35 to 0.40 minutes – 2 %B (modulation time)
Gradient modulation	Constantly shifted %B and Δ%B 2 %B at 0 minutes to 2 %B at 49 minutes to 95 %B at 50 minutes 10 %B at 0.35 minutes to 80 %B at 49 minutes
Temperature	55 °C
Modulation	
Modulation on	4 to 49 minutes
Loops	Two 40 µL loops, cocurrent configuration
Modulation time	0.40 min
Injection	
Volume	8 to 15 µL (UV), 8 µL (MS)
Temperature	4 °C
Needle wash	6 seconds flush port (50 % ACN)
UV Detection	
Wavelength	Signal 214/4 nm, 248/4 nm, 252/4 nm, reference 360/100 nm
Data rate	80 Hz
MS Detection	
Ionization	Agilent Jet Stream technology source, positive ionization
Drying gas	350 °C, 11 L/min
Nebulizer	55 psig
Sheath gas	400 °C, 9 L/min
Capillary voltage	3,500 V
Nozzle voltage	1,000 V
Fragmentor	175 V
Acquisition	Extended dynamic range (2 GHz) Resolution 10,000 for <i>m/z</i> 1,000 MS 8 Spectra All-ions MS/MS 8 Spectra at collision energy 20 or 40 Data dependent MS/MS 8 Spectra MS/MS Threshold (Abs) 1,000 Isolation width ~4 <i>m/z</i> Collision energy (3.6* <i>m/z</i>)/100-4

Software

- Agilent OpenLAB CDS ChemStation revision C.01.07 with 2D-LC add-on software revision A.01.02
- Agilent MassHunter for instrument control (B05.01)
- Agilent MassHunter for data analysis (B07.00)
- Agilent BioConfirm software for MassHunter (B07.00)
- GC Image LC×LC Edition Software for 2D-LC data analysis (GC Image, LLC., Lincoln, NE, USA)

Results and Discussion

Figures 2A and 2B display the UV 214 nm LC×LC tryptic peptide maps of naked trastuzumab (Herceptin) and ado-trastuzumab emtansine (Kadcyla). Orthogonality is mainly directed by the mobile phase pH and the zwitterionic nature of the peptides. A partial correlation that might exist is overruled by the high peak capacity. Using a shifting second-dimension gradient with increasing elution strength as a function of analysis time further increases surface coverage, and, thus, final peak capacity.

Since Herceptin and Kadcyla have the same amino acid sequence, most of the peptide map is identical. Differentiating spots are observed and located in the upper right corner of the plot of Kadcyla, which corresponds to the most hydrophobic part. Since the conjugation of the drugs makes the peptides more hydrophobic, these spots are expected to correspond to the conjugated peptides. The drug has a maximum UV absorbance at 252 nm. Therefore, this wavelength can be used to confirm the positioning of conjugated peptides in the peptide map. As illustrated in Figures 2C and 2D, the upper right corner of the plot becomes more intense in the case of Kadcyla, making this a powerful LC×LC methodology to highlight conjugated peptides.

RPLC×RPLC gradient

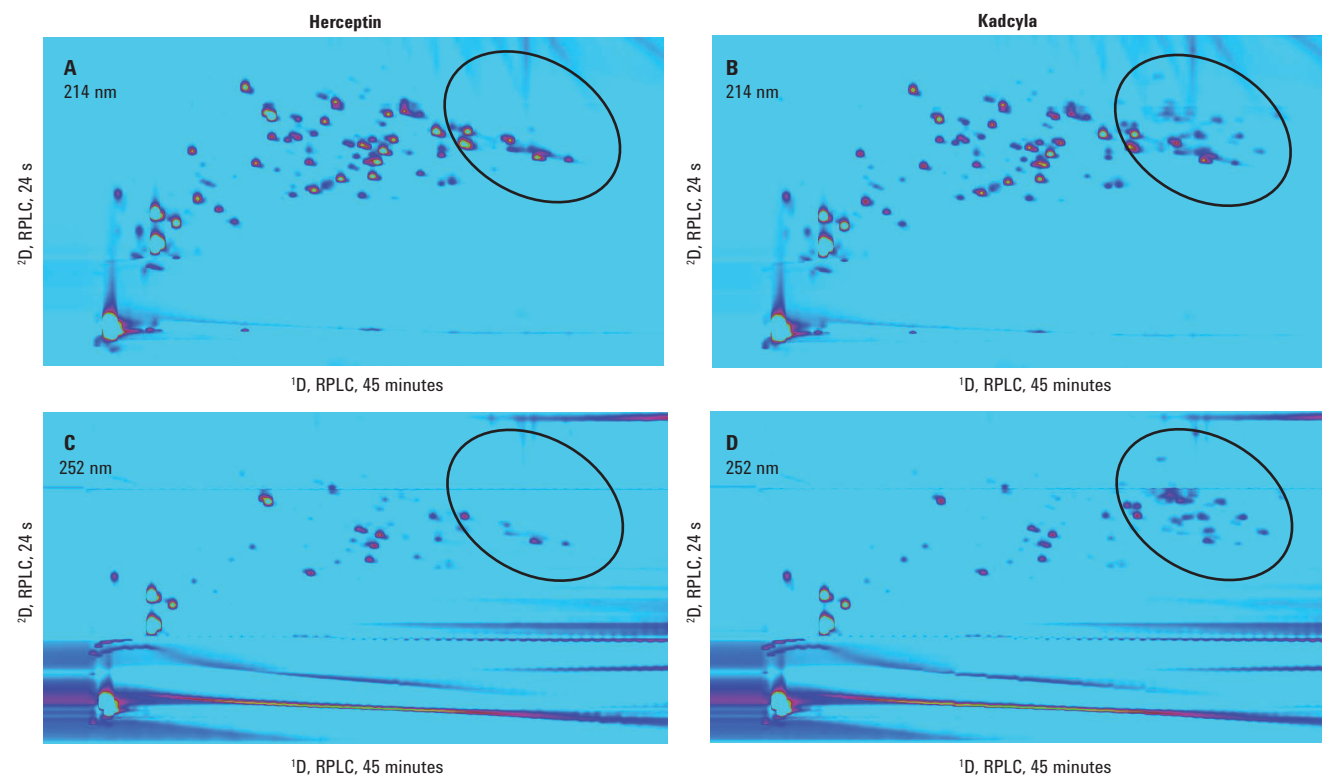
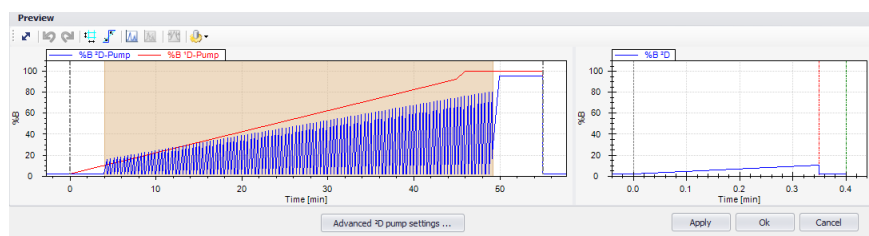


Figure 2. RPLC×RPLC peptide maps of Herceptin (A,C) and Kadcyla (B,D) obtained at 214 and 252 nm UV.

To reveal the identity of these peptides, the RPLC×RPLC methodology was combined with MS and MS/MS. For MS analysis, phosphoric acid was replaced by formic acid as a second-dimension mobile phase additive. Figures 3A and 3B display the RPLC×RPLC-MS tryptic peptide maps of Herceptin and Kadcylya. Table 1 shows a selection of identified conjugated peptides. Figure 4 shows the MS/MS spectrum corresponding to the conjugated peptide TKPR. This spectrum, and by extension all MS/MS spectra associated with DM1 conjugated peptides, are heavily populated by

fragments originating from the drug, for example at m/z 547.2206. Analogous to the UV signal at 252 nm, this ion can be used to recognize conjugated peptides in LC×LC/MS maps. For recognition, the Q-TOF LC/MS system can be operated in all-ions MS/MS mode, which means that the quadrupole is operated in the RF-only mode, thereby transferring all peptides to the collision cell where collision-induced dissociation takes place. As illustrated in Figures 3C, 3D, 3E, and 3F, when extracting from the data the DM1 specific fragment ion at m/z 547.2206 at high mass accuracy,

the upper right corner of the 2D peptide map becomes more intense in the case of Kadcylya in comparison to Herceptin. The latter plot is empty, illustrating the selectivity that is offered by this all-ions MS/MS functionality as opposed to UV detection at 252 nm. Figures 3C and 3D display the all-ions MS/MS data obtained at a collision energy of 20 eV; Figures 3E and 3F show the data at a higher collision energy of 40 eV. Complementary information is obtained when acquiring the data at two different collision energy values.

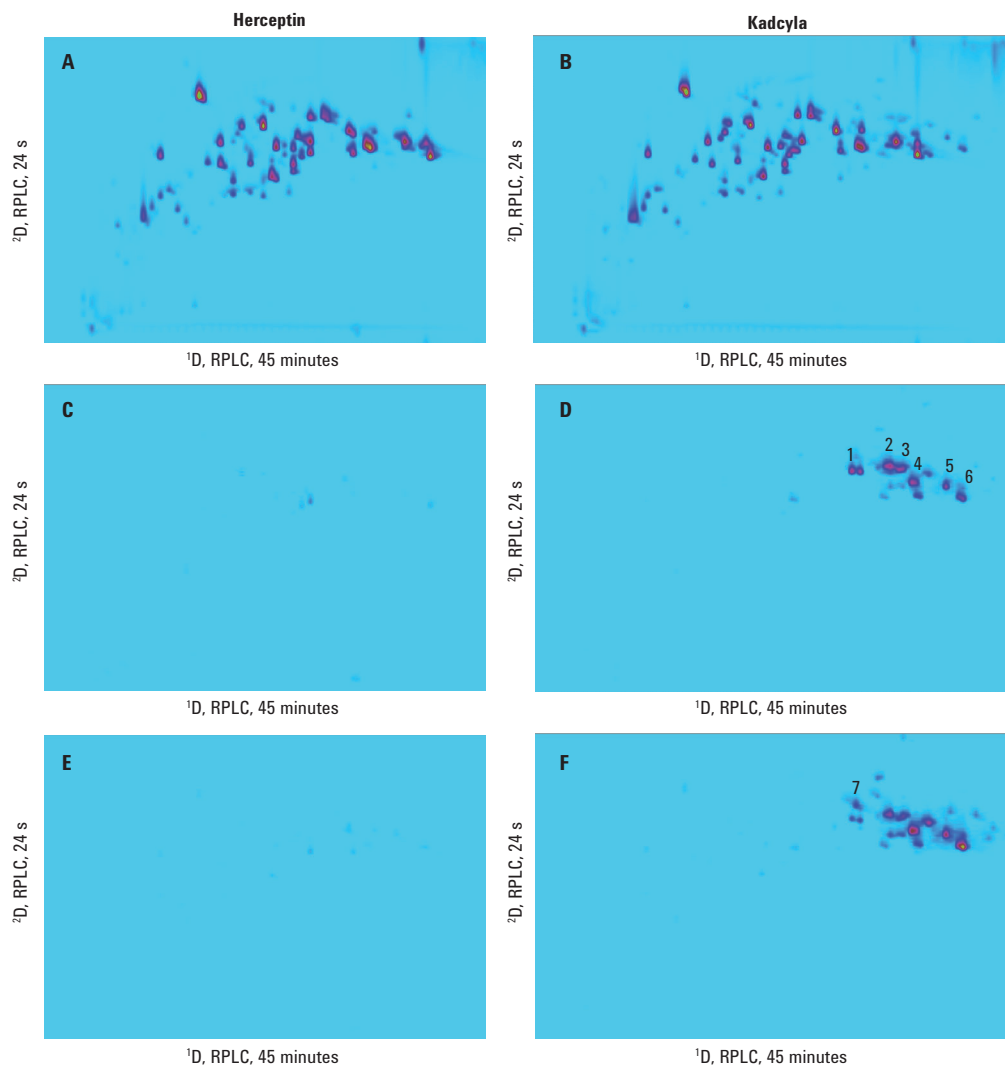


Figure 3. RPLC×RPLC-MS peptide maps of Herceptin (A) and Kadcylya (B) and RPLC×RPLC all ions MS/MS peptide maps of Herceptin (C,E) and Kadcylya (D,F), showing the extracted ion at m/z 547.22056 (extracted at 20 ppm mass accuracy). Collision energy was 20 eV (C,D) and 40 eV (E,F), respectively. Table 1 shows the identities of the annotated spots.

Table 1. A selection of conjugated peptides corresponding to the annotated spots in the LC×LC peptide map shown in Figures 3D and 3F. The conjugated lysine residues are underlined.

No.	Chain	Sequence location	Sequence
1	Lc	184–190	ADYE <u>K</u> HK
2	Hc	292–295	T <u>K</u> PR
3	Hc	413–419	LTVD <u>K</u> SR
4	Hc	222–251	SCD <u>K</u> THTCPPCPAPELLGGPSVFLFPP <u>K</u> PK*
5	Hc	20–38	LSCAASGFN <u>I</u> KDTYIHWVR
6	Hc	305–325	VVSVLTVLHQDWLNG <u>K</u> EY <u>K</u> CK*
7	Hc	259–291	TPRVTCVVVDVSHEDPEV <u>K</u> FNWYVDGVEVHNAK

* Two potential conjugation sites.

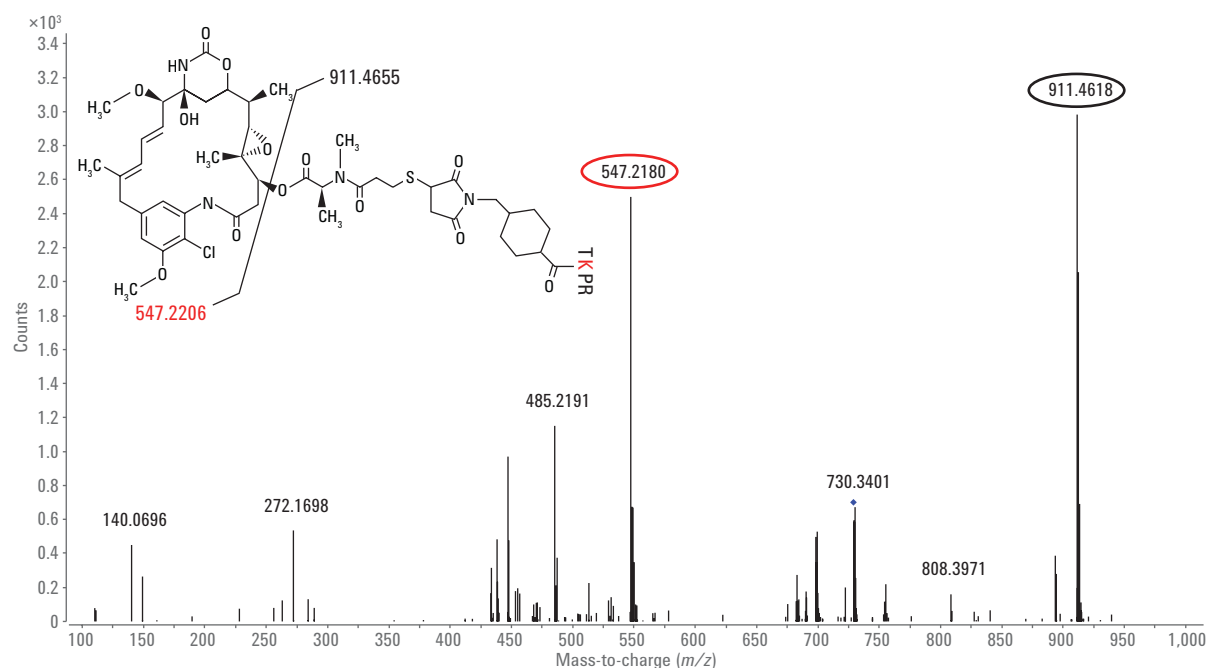


Figure 4. MS/MS spectrum associated with the doubly charged DM1-conjugated peptide TKPR at m/z 729.3411.

A similar strategy was applied to reveal the conjugation sites on brentuximab vedotin (Adcetris), the interchain cysteine-conjugated ADC. With only eight residues (four on each half of the antibody) available for conjugation, Adcetris is much simpler compared to Kadcyla. Figures 5A and 5B display the RPLC×RPLC tryptic peptide maps of Adcetris obtained with UV detection at 214 and 248 nm, the latter wavelength being more selective towards MMAE-conjugated peptides. Three intense spots, located in the upper right corner of the peptide map, become lighter in the 248 nm plot, and are expected to correspond to the conjugated peptides.

Figure 6A displays the RPLC×RPLC/MS tryptic peptide map of Adcetris. The MS/MS spectrum associated with the MMAE-conjugated peptide SCDK is provided in Figure 7. Analogous to DM1-conjugated peptides, MMAE-conjugated peptides also contain specific ions originating from the cytotoxic molecule, that is, at m/z 718.5113. As shown in Figures 6B and 6C, these ions can be extracted from all-ions MS/MS data, enabling recognition of conjugated peptides in the 2D plots. Table 2 shows a selection of identified conjugated peptides. The detection of conjugated intrachain cysteine residues is of particular interest,

exemplified here with heavy-chain peptide NQVSLTCLVK (peak 3 in Figure 6C). These intrachain residues are not targeted during ADC manufacturing. Apparently, the TCEP reduction step is applied to the mAb before conjugation results in collateral intrachain disulfide bridge reduction next to interchain reduction (the latter links are more labile). Resulting free thiol groups can then react with the protease-cleavable linker-MMAE intermediate. These unwanted side products are only detected at trace levels, illustrating the analytical sensitivity of the presented methodology.

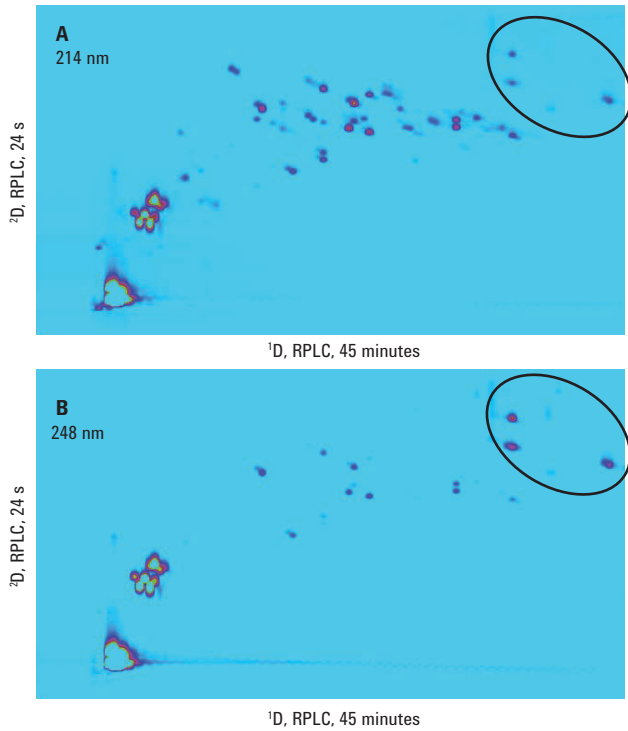


Figure 5. RPLC×RPLC peptide maps of Adcetris obtained at 214 (A) and 248 nm UV (B).

Table 2. A selection of conjugated peptides corresponding to the annotated spots in the LC×LC peptide map shown in Figures 6B and 6C. The conjugated cysteine residues are underlined. Payload: MMAE + linker. Carbamidomethylation results from the alkylation of free cysteine residues with iodoacetamide.

No.	Chain	Sequence location	Sequence
1	Lc	216–218	<u>G</u> <u>E</u> <u>C</u> + payload
2	Hc	219–222	<u>S</u> <u>C</u> <u>D</u> <u>K</u> + payload
3	Hc	361–370	<u>N</u> <u>Q</u> <u>V</u> <u>S</u> <u>L</u> <u>T</u> <u>C</u> <u>L</u> <u>V</u> <u>K</u> + payload
4	Hc	223–248	<u>T</u> <u>H</u> <u>T</u> <u>C</u> <u>P</u> <u>P</u> <u>C</u> <u>P</u> <u>A</u> <u>P</u> <u>E</u> <u>L</u> <u>L</u> <u>G</u> <u>G</u> <u>P</u> <u>S</u> <u>V</u> <u>F</u> <u>L</u> <u>F</u> <u>P</u> <u>P</u> <u>K</u> <u>P</u> <u>K</u> + 1* payload + 1* carbamidomethylation
5	Hc	223–248	<u>T</u> <u>H</u> <u>T</u> <u>C</u> <u>P</u> <u>P</u> <u>C</u> <u>P</u> <u>A</u> <u>P</u> <u>E</u> <u>L</u> <u>L</u> <u>G</u> <u>G</u> <u>P</u> <u>S</u> <u>V</u> <u>F</u> <u>L</u> <u>F</u> <u>P</u> <u>P</u> <u>K</u> <u>P</u> <u>K</u> + 2* payload

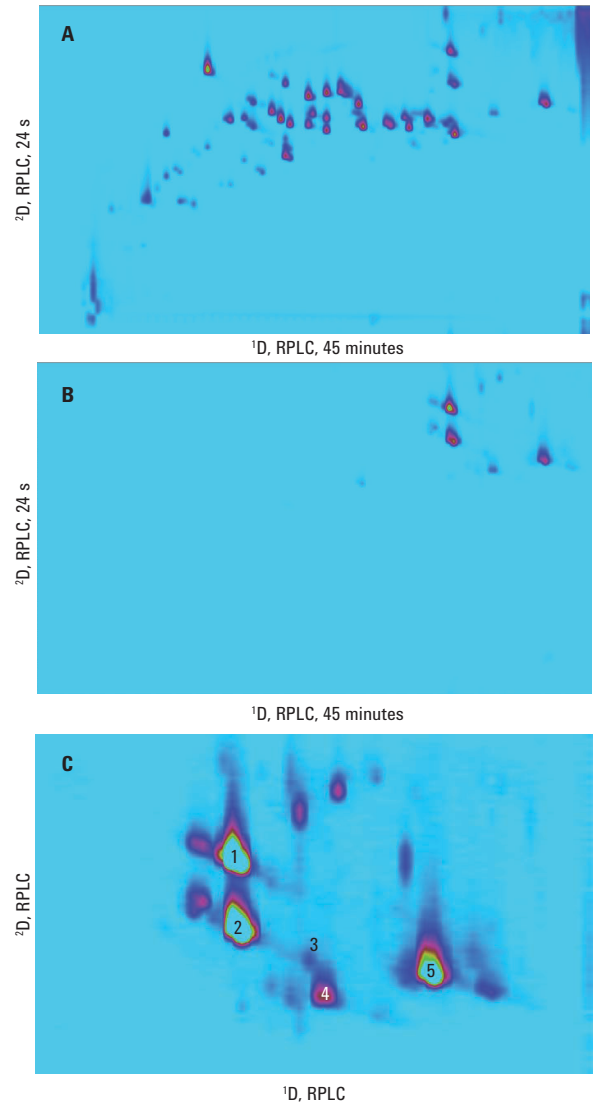


Figure 6. RPLC×RPLC-MS peptide map of Adcetris (A) and RPLC×RPLC all-ions MS/MS peptide map (B,C), showing extracted ion m/z 718.5113 (extracted at 20 ppm mass accuracy). Collision energy was 20 eV. B) Full plot; C) Zoomed intensified plot. Table 2 shows the identity of the annotated spots.

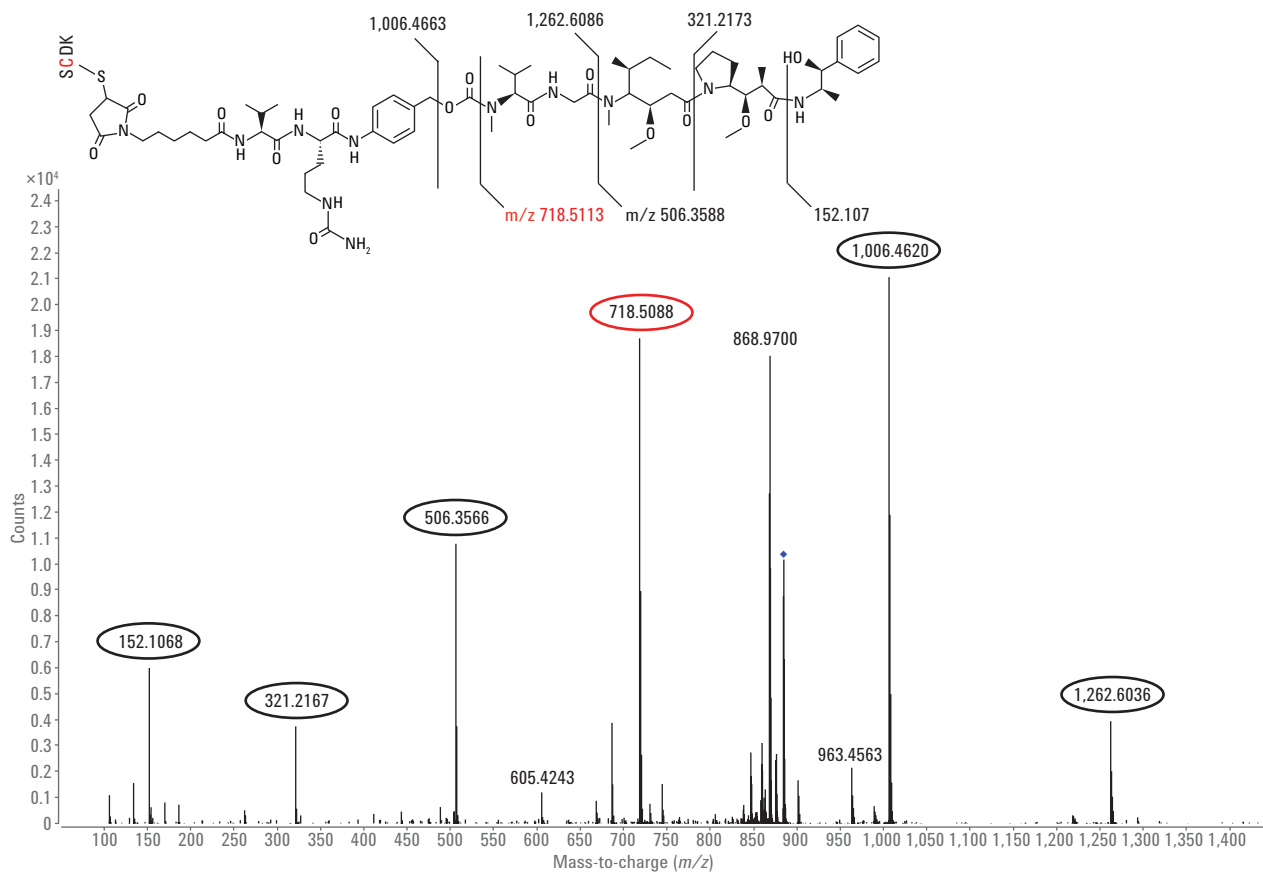


Figure 7. MS/MS spectrum associated with the doubly charged MMAE-conjugated peptide SCDK at m/z 884.4811.

Conclusion

The Agilent 1290 Infinity II 2D-LC Solution combined with an Agilent 6530 Quadrupole Time-of-Flight LC/MS System enables identification of conjugated peptides in ADCs in a highly elegant manner. Considering the robustness of state-of-the-art 2D-LC/MS, these measurements have the potential to be implemented beyond characterization into routine QA/QC environments.

References

1. Sandra, K.; Vandenheede, I.; Sandra, P. Modern chromatographic and mass spectrometric techniques for protein biopharmaceutical characterization, *J. Chromatogr. A* **2014**, *1335*, 81–103.
2. Fekete, S.; *et al.* Chromatographic, electrophoretic and mass spectrometric methods for the analytical characterization of protein biopharmaceuticals, *Anal. Chem.* **2016**, *88*, 480–507.
3. Panowski, S.; *et al.* Site-specific antibody drug conjugates for cancer therapy, *mAbs* **2014**, *6*, 34–45.
4. Wakankar, A.; *et al.* Analytical methods for physicochemical characterization of antibody drug conjugates, *mAbs* **2011**, *3*, 161–172.
5. Beck, A.; Reichert, J. M. Antibody-drug conjugates, *mAbs* **2014**, *6*, 15–17.
6. Sandra, K.; Sandra, P. The opportunities of 2D-LC in the analysis of monoclonal antibodies, *Bioanalysis* **2015**, *7*, 2843–2847.
7. Sandra, K.; *et al.* Multiple heart-cutting and comprehensive two-dimensional liquid chromatography hyphenated to mass spectrometry for the characterization of the antibody-drug conjugate ado-trastuzumab emtansine, *J. Chromatogr. B* **2016**, *1032*, 119–130.
8. Vanhoenacker, G.; *et al.* Comprehensive two-dimensional liquid chromatography of therapeutic monoclonal antibody digests, *Anal. Bioanal. Chem.*, **2015**, *407*, 355–366.
9. Vanhoenacker, G.; *et al.* Analysis of Monoclonal Antibody Digests with the Agilent 1290 Infinity 2D-LC Solution, *Agilent Technologies Application Note*, publication number 5991-2880EN, **2013**.
10. Vanhoenacker, G.; *et al.* Analysis of Monoclonal Antibody Digests with the Agilent 1290 Infinity 2D-LC Solution. Part 2: HILIC×RPLC-MS, *Agilent Technologies Application Note*, publication number 5991-4530EN **2014**.
11. Sandra, K.; *et al.* Identifying monoclonal antibody mutation sites using the Agilent 1290 Infinity II 2D-LC solution combined with Q-TOF LC/MS, *Agilent Technologies Application Note*, publication number 5991-8077EN, **2016**.

www.agilent.com/chem

For Research Use Only. Not for use in diagnostic procedures.

This information is subject to change without notice.

© Agilent Technologies, Inc., 2017
Published in the USA, June 1, 2017
5991-8050EN



Agilent Technologies